Curcumin Ameliorates Skeletal Muscle Atrophy in Type I Diabetic Mice via Inhibiting the Protein Ubiquitination

Taisuke Ono[1]*, Shingo Takada[1]*, Shintaro Kinugawa[1], Tadashi Suga[2], Mochamad A Sobirin[3], Kagami Hirabayashi[1], Masashige Takahashi[1], Arata Fukushima[1], Tsuneaki Homma[1], Takashi Yokota[1], Shouji Matsushima[1], and Hiroyuki Tsutsui[1]

[1] Department of Cardiovascular Medicine, Hokkaido University Graduate School of Medicine, Sapporo, Japan

[2] Faculty of Sport and Health Science, Ritsumeikan University, 1-1-1 Nojihigashi, Kusatsu, Shiga, Japan

[3] Faculty of Medicine, Diponegoro University, Semarang, Indonesia

*These authors contributed equally to this work.

Running title: Curcumin and diabetic skeletal muscle atrophy

Address for Correspondence:

Shintaro Kinugawa, MD, PhD.

Department of Cardiovascular Medicine, Hokkaido University Graduate School of Medicine

Kita-15, Nishi-7, Kita-ku, Sapporo 060-8638, Japan

Phone: +81-11-706-6973, Fax: +81-11-706-7874

E-mail: tuckahoe@med.hokudai.ac.jp

Total number of words, excluding references and figure legends: 3542

Total number of references: 57

New Findings

What is the central question on this study?

We sought to examine whether curcumin could ameliorate skeletal muscle atrophy in diabetic mice by inhibiting protein ubiquitination, inflammatory cytokines and oxidative stress.

What is the main finding and its importance?

We found that curcumin ameliorated skeletal muscle atrophy in streptozotocin-induced diabetic mice by inhibiting protein ubiquitination without affecting protein synthesis. This favorable effect of curcumin was possibly due to the inhibition of inflammatory cytokines and oxidative stress. Curcumin may be beneficial for the treatment of muscle atrophy in type 1 diabetes mellitus.

Abstract

Skeletal muscle atrophy develops in patients with diabetes mellitus (DM), especially in type 1 DM, which is associated with chronic inflammation. Curcumin, the active ingredient of turmeric, has various biological actions including anti-inflammatory and anti-oxidative properties. We thus hypothesized that curcumin could ameliorate skeletal muscle atrophy in streptozotocin (STZ)-induced type 1 DM mice. C57BL/6J mice were injected intraperitoneally with 200 mg/kg of STZ (DM) or vehicle (Control). Each group of mice was randomly divided into 2 groups of 10 mice each and fed a diet with or without curcumin (1500 mg/kg/day) for 2 weeks. There were significant decreases in body weight, skeletal muscle weight, and cellular cross-sectional area of the skeletal muscle in DM mice compared to Controls and they were significantly attenuated in DM+Curcumin without affecting plasma glucose and insulin levels. Ubiquitination of protein was increased in skeletal muscle from DM, and decreased in DM+Curcumin. Gene expressions of muscle-specific ubiquitin E3 ligase Atrogin-1/MAFbx and MuRF1 were increased in DM and inhibited in DM+Curcumin. Moreover, NFκB activation, levels of inflammatory cytokines TNF-α and IL-1β, and oxidative stress were increased in the skeletal muscle from DM and inhibited in DM+Curcumin. Curcumin ameliorated skeletal muscle atrophy in DM mice by inhibiting protein ubiquitination, inflammatory cytokines and oxidative stress. Curcumin may be beneficial for the treatment of muscle atrophy in type 1 DM.

Key words: curcumin, type 1 diabetes, skeletal muscle atrophy, ubiquitin, inflammatory cytokines, oxidative stress, streptozotocin

Introduction

The number of patients with diabetes mellitus (DM) has been increasing steadily in industrialized countries. DM is a major risk factor for atherosclerosis, which increases the incidence of cardiovascular diseases. In addition, various complications can adversely affect the quality of life.

Skeletal muscle atrophy has been reported to be associated with DM, especially type 1 diabetes (T1DM) (Nair *et al.*, 1995; Wang *et al.*, 2006; Frier *et al.*, 2008). Skeletal muscle mass is maintained by the balance between protein synthesis and degradation. Various pathological conditions such as DM, heart failure, cancer, sepsis, acquired immunodeficiency syndrome, severe trauma, uremia and starvation have been reported to cause skeletal muscle atrophy by the disturbance of protein metabolism (Lecker *et al.*, 1999; Hasselgren *et al.*, 2002; Acharyya & Guttridge, 2007). Weight loss associated with skeletal muscle atrophy is tightly associated with increased mortality and decreased exercise capacity, which are major clinical problems (Griffiths, 1996). Skeletal muscle atrophy in these conditions has been caused by protein degradation pathways, especially the ubiquitin-proteasome (UP) system (Lecker *et al.*, 1999; Hasselgren *et al.*, 2002; Acharyya & Guttridge, 2007). Ubiquitin binds to the substrate of targeted proteins via the ubiquitin-activating enzyme (E1), ubiquitin-conjugating enzyme (E2), and ubiquitin ligase enzymes (E3), which activate the proteolytic signaling pathway (Mitch & Goldberg, 1996). Among them, E3 ubiquitin ligases have substrate specificity, and gene expressions of Atrogin-1/MAFbx and MuRF1 in the skeletal muscle have been reported to be increased during the atrophy process (Bodine *et al.*, 2001a; Gomes *et al.*, 2001; Wray *et al.*, 2003). Moreover, numerous studies have reported that activation of NFκB and FoxO increased Atrogin-1/MAFbx and MuRF1 in a muscle atrophy model (Kelleher *et al.*, 2010; Hulmi *et al.*, 2012; Lv *et al.*, 2014). Elevations of inflammatory cytokines and oxidative stress have been suggested to be involved in the activation of protein degradation (Mastrocola *et al.*, 2008). On the other hand, insulin and insulin-like growth factor (IGF)-1 promote the phosphorylation of the Akt/mammalian target of rapamycin (mTOR) and activate protein synthesis, which is known to be involved in suppression of the UP system. These deficiencies or reduced reactivity are thought to be involved in skeletal muscle atrophy (Dehoux *et al.*, 2004).

Skeletal muscle atrophy has been found in streptozotocin (STZ)-induced T1DM mice (Mastrocola *et al.*, 2008; Chen *et al.*, 2009), and was shown to be inhibited by insulin (Chen *et al.*, 2009) or dehydroepiandrosterone (Mastrocola *et al.*, 2008). Curcumin, a component of spice turmeric (Curcuma longa), is widely used in Asia as a traditional herbal medicine (Corson & Crews, 2007). It is used for the treatment of various diseases, such as respiratory and liver diseases, anorexia, and arthritis, and also has antitumor activity (Corson & Crews, 2007; Epstein *et al.*, 2010). This compound can inhibit inflammatory cytokines and oxidative stress, and suppresses nuclear factor-kappa B (NFκB) (Jobin *et al.*, 1999; Sharma *et al.*, 2007; Poylin *et al.*, 2008; Tikoo *et al.*, 2008; Chiu *et al.*, 2009). Therefore, curcumin has been expected to have an inhibitory effect on skeletal muscle atrophy (Busquets *et al.*, 2001; Jin & Li, 2007). However, the effect of curcumin against diabetic skeletal muscle atrophy has never been explored. Thus, in this study we assessed the inhibitory effect of curcumin on skeletal muscle atrophy in T1DM mice.

Materials and Methods

Experimental animals

The study was approved by our institutional animal research committee and conformed to the animal care guidelines for the Care and Use of Laboratory Animals in Hokkaido University Graduate School of Medicine.

Male C57BL/6J mice (8–10 weeks of age, total n=40) were purchased from CLEA Japan (Tokyo, Japan), housed under pathogen-free conditions, and fed on a standard chow diet (CE-2, CLEA Japan). DM was induced in mice by intraperitoneal injection of STZ (Sigma-Aldrich, St. Louis, MO, USA; 200 mg/kg body weight) dissolved in citrate buffer (50 mM; pH 4.5) as previously described (Lu *et al.*, 1998; Lesniewski *et al.*, 2003). It has been shown that this protocol can effectively induce diabetic status and skeletal muscle atrophy in mice (Lesniewski *et al.*, 2003; Chen *et al.*, 2009; Whitman *et al.*, 2013; Wang *et al.*, 2015). It has also been reported that pancreatic islet transplantation reverses the diabetic effects of high-dose STZ in mice, which suggests that the pathology results from diabetes itself and not from secondary effects of the drug (Chen *et al.*, 2009). As a control, only citrate buffer was injected. Blood glucose concentration was assessed using a glucometer (Glutest Ace R; Sanwa Kagaku Kenkyusho, Nagoya, Japan) from the tail vein after 3 days to confirm that glucose levels greater than 300 mg/dl were reached by STZ injection.

Each group of mice was randomly divided into two groups with or without curcumin (LKT laboratories, St. Paul, Minnesota; 1500 mg/kg body weight/day) in their chow. In previous reports using rodents, curcumin was administered over a wide range of doses, 10–2000 mg/kg/day (Anand *et al.*, 2007). In our preliminary experiments, we used 3 different doses of curcumin, 150, 450, and 1500 mg/kg/day, and found an inhibitory effect of skeletal muscle atrophy only for 1500 mg/kg/day. Therefore, a dose of 1500 mg/kg/day was added to the chow of the Control+Curcumin and DM+Curcumin groups while the Control and DM groups received none. The quantities of chow consumed by each group of mice (Control: 3.3±0.3 vs. Control+Curcumin: 3.3±0.8 vs. DM: 3.1±0.2 vs. DM+Curcumin: 2.9±0.1 g/day/mouse) and body weight were monitored every 3 days, and the rate of curcumin in the chow was adjusted to ensure a consistent daily dose.

Plasma glucose and insulin

After animals fasted for 6 h, blood samples were collected from the inferior vena cava. The glucose concentration was measured using Glucose Assay kit (Bio Chain, Hayward, CA, USA) and insulin was measured using Insulin enzyme-linked immunosorbent assay (ELISA) kit (Morinaga Institute of Biochemical Science, Kanagawa, Japan) after 2 weeks of STZ injection.

NFκB activation assay

Muscle NFκB was measured using TransAM™ NFκB Transcription Factor Assay Kits (Active Motif®, CA, USA) according to the manufacturer's instructions, as previously described (Du *et al.*, 2013).

Tissue preparation and histology

Hindlimb skeletal muscle was excised and weighed under deep anesthesia with Avertin (250 mg/kg body weight). The total skeletal muscle (rectus femoris, gastrocnemius, and soleus) was isolated and weighed. Skeletal muscle tissues were fixed in 10% formaldehyde, and paraffin sections were stained with hematoxylin and eosin using standard techniques. Myocyte cross-sectional areas in the gastrocnemius muscle were determined for at least 150 fibers/animal. Image J software (NIH) was used for these analyses (Takada *et al.*, 2013).

Immunoblotting in the skeletal muscle

Other skeletal muscle tissue samples were snap-frozen into liquid nitrogen immediately after harvesting and stored at -80 °C until further analysis. All immunoblotting was performed within 1 month after sampling from mice. Ubiquitinated protein was determined by performing immunoblotting using the ubiquitin antibody (Cell Signaling Technology, MA, USA) as described previously (Paul *et al.*, 2012).

Immunoblotting was performed using antibodies against the following: phosphorylation of Akt at Ser473 and Thr308, phosphorylation of mTOR at Ser2448, phosphorylation of p70S6K at Thr389, phosphorylation of forkhead box O (FoxO)3a at Ser253, cleaved caspase-3, autophagy-related gene

(Atg)12-Atg5, LC3II (Cell Signaling) and phosphorylation of FoxO3a at Thr32, phosphorylation of Akt at Thr308 (Abcam, MA, USA), p70S6K, and myostatin (Santa Cruz Biotechnology, Santa Cruz, CA). Equal amounts of protein extracted from skeletal muscle tissues were used, as described previously (Takada *et al.*, 2013; Fukushima *et al.*, 2014; Takada *et al.*, 2014; Kadoguchi *et al.*, 2015). Values were expressed as the ratio of target band intensity to the internal control intensity. GAPDH (Cell Signaling) was used as an internal control to normalize results and to control for blot-to-blot variation.

Quantitative reverse transcriptase polymerase chain reaction

Total RNA was extracted from the skeletal muscle with QuickGene-810 (FujiFilm, Tokyo, Japan) according to the manufacturer's instructions. Complementary DNA (cDNA) was synthesized with the high-capacity cDNA reverse transcription kit (Applied Biosystems, CA, USA). TaqMan quantitative polymerase chain reaction (PCR) was performed with the 7300 real-time PCR system (Applied Biosystems, CA, USA) to amplify samples for Atrogin-1/Muscle Atrophy F-box (MAFbx) (Mm00499523_m1), Muscle Ring Finger 1 (MuRF1) (Mm0118522_m1), tumor necrosis factor (TNF)-α (Mm0043258_m1), and interleukin (IL)-1β (Mm00434228_m1) cDNA in the skeletal muscle. These transcripts were normalized to GAPDH as an internal control. The primers were purchased from Applied Biosystems. Data were analyzed using the comparative $2^{-\Delta\Delta CT}$ method as described previously (Takada *et al.*, 2013; Fukushima *et al.*, 2014; Suga *et al.*, 2014; Nishikawa *et al.*, 2015).

O_2^- production and tiobarbituric acid reactive substances (TBARS)

The chemiluminescence elicited by O_2^- in the presence of lucigenin (5 μmol/L) was measured in hindlimb skeletal muscle using a luminometer (AccuFLEX Lumi 400; Aloka, Tokyo, Japan) as previously described (Takada *et al.*, 2013; Fukushima *et al.*, 2014; Suga *et al.*, 2014; Takada *et al.*, 2014; Kadoguchi *et al.*, 2015; Nishikawa *et al.*, 2015). To validate that the chemiluminescence signals were derived from O_2^-, measurements were also performed in the presence of Tiron (20 mmol/L), a cell-permeating, nonenzymatic scavenger of O_2^-. The degree of lipid peroxidation in the skeletal muscle was determined though a biochemical assay of malondialdehyde formation [thiobarbituric acid

188 reactive substances (TBARS) assay kit; Cayman Chemical, Ann Arbor, MI], according to the
189 manufacturer's protocol as previously described (Takada *et al.*, 2013; Suga *et al.*, 2014).
190
191 **Circulating and muscle IGF-1**
192 Circulating and muscle IGF-1 were measured using an IGF-1 ELISA kit (R&D system®, MN,
193 USA) according to the manufacturer's instructions.
194
195 **Serum TNF-α and IL-1β**
196 Serum TNF-α and IL-1β were measured using TNF-α and IL-1β ELISA kit (R&D system)
197 according to the manufacturer's instructions.
198
199 **Statistical analysis**
200 Statistical analyses were performed using PASW statistics software (IBM, Armonk, NY,
201 USA). Data are expressed as means ± standard errors (SEM). For multiple-group comparisons, two-
202 way analysis of variance (ANOVA) was performed, followed by Tukey's test. $P<0.05$ was considered
203 statistically significant.
204

Results

Plasma glucose, insulin and body weight

Blood glucose and body weight before STZ injection were comparable among the 4 groups (data not shown). There were no significant differences in blood glucose level at 3 days after STZ injection between DM and DM+Curcumin mice (480±17 vs. 480±22 mg/dl, p=NS). Plasma glucose level was significantly increased and insulin level was significantly decreased in DM mice compared to Control mice (**Figure 1A and B**). Change in body weight after 14 days was significantly larger in DM mice than Control mice (**Figure 1C**). The diet with curcumin in DM mice significantly attenuated changes in body weight without affecting plasma glucose and insulin level (**Figure 1A-C**).

Skeletal muscle weight and myocyte cross-sectional area

In parallel with the changes in body weight, the significant reductions in the rectus femoris and gastrocnemius muscle weights in DM mice were attenuated by the treatment with curcumin (**Figure 1D, E**). There was no significant difference in the soleus muscle weight among the groups (**Figure 1F**). The myocyte cross-sectional area of gastrocnemius muscle was significantly smaller in DM mice than Control mice, and was partially improved in DM+Curcumin (**Figure 1G, H**).

Ubiqutin-conjugated protein and ubiquitin E3 ligase in the skeletal muscle

Ubiquitin-conjugated proteins are shown as smears at their molecular weights (**Figure 2A**). They were significantly increased in DM mice compared to Control mice, and were significantly decreased in DM+Curcumin mice (**Figure 2B**).

Gene expressions of muscle-specific E3 ubiquitin ligases, Atrogin-1/MAFbx and MuRF1, were measured using real-time RT-PCR (**Figure 2C, D**). These mRNA expressions were significantly increased in DM mice compared to Control mice, and were significantly decreased in DM+Curcumin mice.

Inflammatory cytokines in the skeletal muscle and serum

Gene expressions of TNF-α and IL-1β were significantly increased in DM mice compared to Control mice, an effect that was significantly suppressed in DM+Curcumin mice (**Figure 3A, B**). Likewise, serum TNF-α and IL-1β were significantly increased in DM mice compared to Control mice, but did not differ between DM and DM+Curcumin mice (**Figure 3C, D**).

Oxidative stress in the skeletal muscle

O_2^- production and TBARS were significantly increased in DM mice compared to Control mice; these effect were significantly inhibited in DM+Curcumin mice (**Figure 3E, F**).

NFκB and FoxO3a activation in the skeletal muscle

NFκB p65 activation was significantly increased in DM mice compared to Control mice, but not in DM+Curcumin mice (**Figure 4A**). Phosphorylation of FoxO3a at serine 253 but not threonine 32 was significantly decreased in DM mice compared to Control mice, and did not differ between DM and DM+Curcumin mice (**Figure 4B, C**).

Apoptosis and autophagy-related protein in the skeletal muscle

The expressions of apoptosis-related molecules, cleaved caspase-3, autophagy-related molecules, Atg12-Atg5, and LC3II were significantly increased in DM mice, and did not differ between DM and DM+Curcumin mice (**Figure 4D-F**).

Protein synthesis in the skeletal muscle

Circulating and skeletal muscle IGF-1 levels were significantly decreased in DM mice compared to Control mice, and did not differ between DM and DM+Curcumin mice (**Figure 5A, B**). **Figure 5C** shows representative bands of protein synthesis-related protein. Similarly, phosphorylation of Akt at serine 473 and threonine 308, mTOR at serine 2448, p70S6K at threonine 389, total and p70S6K were decreased, and myostatin was increased in DM mice compared to Control mice (**Figure 5D-I**). These values did not differ between DM and DM+Curcumin mice (**Figure 5D-I**).

Discussion

The most important finding of this study was that curcumin prevented skeletal muscle atrophy in an STZ-induced T1DM model. Furthermore, curcumin inhibited the DM-related increase in gene expression of E3 ubiquitin ligases and the concomitant increase in ubiquitinated protein in the skeletal muscle, without affecting insulin level and protein synthesis signaling. Curcumin also inhibited NFκB activation, the gene expression of inflammatory cytokines, and oxidative stress in the skeletal muscle. Therefore, the inhibitory effect of curcumin on skeletal muscle atrophy was due to the inhibition of the UP system via regulation of inflammation and oxidative stress.

Oxidative stress has been reported to be increased in STZ-induced DM, which is also associated with the development of muscle atrophy (Li *et al.*, 2003; Bechara *et al.*, 2014; Pal *et al.*, 2014). Furthermore, oxidative stress was shown to induce increases in ubiquitin-conjugating activity and muscle-specific ubiquitin ligase Atrogin-1/MAFbx and MuRF1 in C2C12 murine myoblasts (Li *et al.*, 2003). In the present study, O_2^- production and TBRAS in the skeletal muscle were significantly increased in DM mice compared to Control mice, an effect that was significantly suppressed by curcumin (**Figure 3E, F**). Therefore, our data suggest that the favorable effects of curcumin may be due to an anti-oxidant property (**Figure 3E, F**). On the other hand, proinflammatory cytokines such as TNF-α and IL-1β have been reported to be major factors causing skeletal muscle atrophy (Argiles & Lopez-Soriano, 1999; Li *et al.*, 2009). It has been reported that TNF-α and IL-1β are involved in skeletal muscle atrophy by activation of NFκB, which induces upregulation of ubiquitin ligase E3 (von Haehling *et al.*, 2002; Cai *et al.*, 2004). Li et al. reported that an increase in protein catabolism by TNF-α was suppressed by inhibition of NFκB in C2C12 mouse skeletal myotubes (Li & Reid, 2000). Moreover, inflammatory cytokines are known to express and accelerate O_2^- production in the skeletal muscle ((Plomgaard *et al.*, 2005; Liao *et al.*, 2010; Zuo *et al.*, 2014). In contrast, ROS is known to induce inflammation in the skeletal muscle (Allen & Tresini, 2000). In the present study, gene expressions of TNF-α and IL-1β, and NFκB activation as well as O_2^- production and TBRAS in the skeletal muscle were significantly increased in DM mice compared to Control mice; this effect was significantly suppressed by curcumin (**Figure 3C-F, and Figure 4A**). These results support previous study that curcumin has anti-oxidant and anti-inflammatory properties in the skeletal muscle (Avci *et*

al., 2012). While, serum TNF-α and IL-1β levels were significantly increased in DM mice compared to Control mice, but did not improve by curcumin (**Figure 3C, D**). Therefore, curcumin may inhibits protein degradation through directly suppress ROS production and/or indirectly inhibits accelerated it by inhibiting cytokines expression in the skeletal muscle from DM mice (**Figure 1, Figure 3 and Figure 4**).

Apoptotic cell death and autophagy also play crucial roles in the development of skeletal muscle atrophy. Busquets *et al.* have reported increased apoptosis in the skeletal muscle of patients with cancer cachexia (Busquets *et al.*, 2007). It has been reported that an apoptosis-inhibiting factor inhibited the increased proteolysis in the skeletal muscle in STZ-induced T1DM mice (Wang *et al.*, 2007). Lv et al. reported that autophagy was increased in skeletal muscle in STZ-induced diabetic mice (Lv *et al.*, 2014). Therefore, we also examined the involvement of apoptosis and autophagy in skeletal muscle atrophy. However, the apoptosis-related protein cleaved caspase-3, the autophagy-related protein Atg12-Atg5, and LC3II were increased in the skeletal muscle from both DM and DM+Curcumin mice, with no differences between groups (**Figure 4**). Therefore, there was almost no participation of apoptosis and autophagy in the protection of skeletal muscle atrophy by curcumin in the present study.

The balance between protein synthesis and protein degradation maintains skeletal muscle mass. The stimulation of muscle hypertrophy, such as weight load, increases muscle protein synthesis and induces muscle hypertrophy; in contrast, catabolic diseases increase protein degradation and cause muscle atrophy. Insulin and IGF-1 are involved in protein synthesis by stimulating Akt/mTOR and their downstream targets (Bodine *et al.*, 2001b; Rommel *et al.*, 2001). Blood insulin, IGF-I, and muscle IGF-1 levels were remarkably reduced in DM mice compared to Control mice and were not affected by curcumin (**Figure 1B, Figure 5A, B**). The changes in phosphorylated Akts, mTOR, p70S6K, total p70S6K and myostatin levels were consistent with the changes in insulin level (**Figure 5C-I**). Therefore, STZ-induced muscle atrophy was due to the deterioration of protein synthesis as well as the enhancement of protein degradation; however, the inhibitory effect of curcumin was mainly due to the inhibition of protein degradation.

There are several limitations that should be acknowledged in the present study. First, we could not verify whether the dose of curcumin used in the present study (1500 mg/kg/day) was appropriate for preventing muscle atrophy. In a previous study, curcumin was tested at various doses ranging from 10 to 2000 mg/kg/day (Anand *et al.*, 2007). It is known that high doses of curcumin are well tolerated and safe (Lao *et al.*, 2006). Second, we could not exclude the possibility that curcumin directly inhibited protein ubiquitination but not inflammation and oxidative stress. Finally, previous study has reported that curcumin has anti-oxidants properties (Avci *et al.*, 2012), although detailed mechanisms has never been clarified. In the present study, we also could not define it. Further experiments are needed to clarify this issue.

Curcumin ameliorated skeletal muscle atrophy in STZ-induced T1DM mice via inhibiting protein ubiquitination, but not by affecting protein synthesis. Curcumin may be beneficial for the treatment of muscle atrophy in T1DM.

Author contributions

T.O. and S.T. designed experiments, performed experiments, analyzed data, and wrote the manuscript. K. S. conceived and designed experiments, and wrote the manuscript. T.S., A.F., T.H. performed experiments, and analyzed data. M.T., S.M.A., K.H., T.Y. and S.M. contributed to discussion. H.T. designed experiments, contributed to discussion, reviewed and edited the manuscript. All authors have read and approved the manuscript.

Fundings

This study was supported by grants from the Ministry of Education, Culture, Sports, Science and Technology (24390192, 25893005, 26350879, 26750331), Banyu Life Science Foundation International, Suzuken Memorial Foundation, and Takeda Science Foundation.

Acknowledgments

We thank Kaoruko Kawai, Akiko Aita, Miwako Fujii, Yuki Kimura, and Noriko Ikeda for

342 technical assistance in the experiments.

343

344 **Competing interest**

345 None.

346
347

348 **References**

349 Acharyya S & Guttridge DC (2007). Cancer cachexia signaling pathways continue to emerge yet
350 much still points to the proteasome. *Clin Cancer Res* 13, 1356-1361.
351
352 Allen RG & Tresini M (2000). Oxidative stress and gene regulation. *Free Radic Biol Med* 28, 463-499.
353
354 Anand P, Kunnumakkara AB, Newman RA & Aggarwal BB (2007). Bioavailability of curcumin:
355 problems and promises. *Mol Pharm* 4, 807-818.
356
357 Argiles JM & Lopez-Soriano FJ (1999). The role of cytokines in cancer cachexia. *Med Res Rev* 19,
358 223-248.
359
360 Avci G, Kadioglu H, Sehirli AO, Bozkurt S, Guclu O, Arslan E & Muratli SK (2012). Curcumin
361 protects against ischemia/reperfusion injury in rat skeletal muscle. *J Surg Res* 172, e39-46.
362
363 Bechara LR, Moreira JB, Jannig PR, Voltarelli VA, Dourado PM, Vasconcelos AR, Scavone C,
364 Ramires PR & Brum PC (2014). NADPH oxidase hyperactivity induces plantaris atrophy in
365 heart failure rats. *Int J Cardiol* 175, 499-507.
366
367 Bodine SC, Latres E, Baumhueter S, Lai VK, Nunez L, Clarke BA, Poueymirou WT, Panaro FJ, Na E,
368 Dharmarajan K, Pan ZQ, Valenzuela DM, DeChiara TM, Stitt TN, Yancopoulos GD & Glass
369 DJ (2001a). Identification of ubiquitin ligases required for skeletal muscle atrophy. *Science*
370 294, 1704-1708.
371
372 Bodine SC, Stitt TN, Gonzalez M, Kline WO, Stover GL, Bauerlein R, Zlotchenko E, Scrimgeour A,
373 Lawrence JC, Glass DJ & Yancopoulos GD (2001b). Akt/mTOR pathway is a crucial
374 regulator of skeletal muscle hypertrophy and can prevent muscle atrophy in vivo. *Nat Cell*
375 *Biol* 3, 1014-1019.

Busquets S, Carbo N, Almendro V, Quiles MT, Lopez-Soriano FJ & Argiles JM (2001). Curcumin, a natural product present in turmeric, decreases tumor growth but does not behave as an anticachectic compound in a rat model. *Cancer Lett* 167, 33-38.

Busquets S, Deans C, Figueras M, Moore-Carrasco R, Lopez-Soriano FJ, Fearon KC & Argiles JM (2007). Apoptosis is present in skeletal muscle of cachectic gastro-intestinal cancer patients. *Clin Nutr* 26, 614-618.

Cai D, Frantz JD, Tawa NE, Jr., Melendez PA, Oh BC, Lidov HG, Hasselgren PO, Frontera WR, Lee J, Glass DJ & Shoelson SE (2004). IKKbeta/NF-kappaB activation causes severe muscle wasting in mice. *Cell* 119, 285-298.

Chen Y, Cao L, Ye J & Zhu D (2009). Upregulation of myostatin gene expression in streptozotocin-induced type 1 diabetes mice is attenuated by insulin. *Biochem Biophys Res Commun* 388, 112-116.

Chiu J, Khan ZA, Farhangkhoee H & Chakrabarti S (2009). Curcumin prevents diabetes-associated abnormalities in the kidneys by inhibiting p300 and nuclear factor-[kappa]B. *Nutrition* 25, 964-972.

Corson TW & Crews CM (2007). Molecular understanding and modern application of traditional medicines: triumphs and trials. *Cell* 130, 769-774.

Dehoux M, Van Beneden R, Pasko N, Lause P, Verniers J, Underwood L, Ketelslegers JM & Thissen JP (2004). Role of the insulin-like growth factor I decline in the induction of atrogin-1/MAFbx during fasting and diabetes. *Endocrinology* 145, 4806-4812.

Du X, He S, Jiang Y, Wei L & Hu W (2013). Adiponectin prevents islet ischemia-reperfusion injury through the COX2-TNFalpha-NF-kappaB-dependent signal transduction pathway in mice. *J Endocrinol* 218, 75-84.

Epstein J, Sanderson IR & MacDonald TT (2010). Curcumin as a therapeutic agent: the evidence from in vitro, animal and human studies. *Br J Nutr* 103, 1545-1557.

Frier BC, Noble EG & Locke M (2008). Diabetes-induced atrophy is associated with a muscle-specific alteration in NF-kappaB activation and expression. *Cell Stress Chaperon* 13, 287-296.

Fukushima A, Kinugawa S, Takada S, Matsushima S, Sobirin MA, Ono T, Takahashi M, Suga T, Homma T, Masaki Y, Furihata T, Kadoguchi T, Yokota T, Okita K & Tsutsui H (2014). (Pro)renin receptor in skeletal muscle is involved in the development of insulin resistance associated with postinfarct heart failure in mice. *Am J Physiol Endocrinol Metab* 307, E503-514.

Gomes MD, Lecker SH, Jagoe RT, Navon A & Goldberg AL (2001). Atrogin-1, a muscle-specific F-box protein highly expressed during muscle atrophy. *Proc Natl Acad Sci U S A* 98, 14440-14445.

Griffiths RD (1996). Muscle mass, survival, and the elderly ICU patient. *Nutrition* 12, 456-458.

Hasselgren P-O, Wray C & Mammen J (2002). Molecular Regulation of Muscle Cachexia: It May Be More Than the Proteasome. *Biochem Biophys Res Commun* 290, 1-10.

Hulmi JJ, Silvennoinen M, Lehti M, Kivela R & Kainulainen H (2012). Altered REDD1, myostatin, and Akt/mTOR/FoxO/MAPK signaling in streptozotocin-induced diabetic muscle atrophy. *Am J Physiol Endocrinol Metab* 302, E307-315.

Jin B & Li YP (2007). Curcumin prevents lipopolysaccharide-induced atrogin-1/MAFbx upregulation and muscle mass loss. *J Cell Biochem* 100, 960-969.

Jobin C, Bradham CA, Russo MP, Juma B, Narula AS, Brenner DA & Sartor RB (1999). Curcumin blocks cytokine-mediated NF-kappa B activation and proinflammatory gene expression by inhibiting inhibitory factor I-kappa B kinase activity. *J Immunol* 163, 3474-3483.

Kadoguchi T, Kinugawa S, Takada S, Fukushima A, Furihata T, Homma T, Masaki Y, Mizushima W, Nishikawa M, Takahashi M, Yokota T, Matsushima S, Okita K & Tsutsui H (2015). Angiotensin II can directly induce mitochondrial dysfunction, decrease oxidative fibre number and induce atrophy in mouse hindlimb skeletal muscle. *Exp Physiol* 100, 312-322.

Kelleher AR, Fairchild TJ & Keslacy S (2010). STZ-induced skeletal muscle atrophy is associated with increased p65 content and downregulation of insulin pathway without NF-kappaB canonical cascade activation. *Acta Diabetol* 47, 315-323.

Lao CD, Ruffin MTt, Normolle D, Heath DD, Murray SI, Bailey JM, Boggs ME, Crowell J, Rock CL & Brenner DE (2006). Dose escalation of a curcuminoid formulation. *BMC Complement Altern Med* 6, 10.

Lecker SH, Solomon V, Mitch WE & Goldberg AL (1999). Muscle protein breakdown and the critical role of the ubiquitin-proteasome pathway in normal and disease states. *J Nutr* 129, 227S-237S.

Lesniewski LA, Miller TA & Armstrong RB (2003). Mechanisms of force loss in diabetic mouse skeletal muscle. *Muscle Nerve* 28, 493-500.

459 Li W, Moylan JS, Chambers MA, Smith J & Reid MB (2009). Interleukin-1 stimulates catabolism in
460 C2C12 myotubes. *Am J Physiol Cell Physiol* 297, C706-714.
461
462 Li YP, Chen Y, Li AS & Reid MB (2003). Hydrogen peroxide stimulates ubiquitin-conjugating
463 activity and expression of genes for specific E2 and E3 proteins in skeletal muscle myotubes.
464 *Am J Physiol Cell Physiol* 285, C806-812.
465
466 Li YP & Reid MB (2000). NF-kappaB mediates the protein loss induced by TNF-alpha in
467 differentiated skeletal muscle myotubes. *Am J Physiol Regul Integr Comp Physiol* 279,
468 R1165-1170.
469
470 Liao P, Zhou J, Ji LL & Zhang Y (2010). Eccentric contraction induces inflammatory responses in rat
471 skeletal muscle: role of tumor necrosis factor-alpha. *Am J Physiol Regul Integr Comp Physiol*
472 298, R599-607.
473
474 Lu WT, Juang JH, Hsu BR & Huang HS (1998). Effects of high or low dose of streptozocin on
475 pancreatic islets in C57BL/6 and C.B17-SCID mice. *Transplant Proc* 30, 609-610.
476
477 Lv P, Huang J, Yang J, Deng Y, Xu J, Zhang X, Li W, Zhang H & Yang Y (2014). Autophagy in
478 muscle of glucose-infusion hyperglycemia rats and streptozotocin-induced hyperglycemia rats
479 via selective activation of m-TOR or FoxO3. *PLoS One* 9, e87254.
480
481 Mastrocola R, Reffo P, Penna F, Tomasinelli CE, Boccuzzi G, Baccino FM, Aragno M & Costelli P
482 (2008). Muscle wasting in diabetic and in tumor-bearing rats: role of oxidative stress. *Free*
483 *Radic Biol Med* 44, 584-593.
484
485 Mitch WE & Goldberg AL (1996). Mechanisms of Muscle Wasting -- The Role of the Ubiquitin-
486 Proteasome Pathway. *N Engl J Med* 335, 1897-1905.

Nair KS, Ford GC, Ekberg K, Fernqvist-Forbes E & Wahren J (1995). Protein dynamics in whole body and in splanchnic and leg tissues in type I diabetic patients. *J Clin Invest* 95, 2926-2937.

Nishikawa M, Ishimori N, Takada S, Saito A, Kadoguchi T, Furihata T, Fukushima A, Matsushima S, Yokota T, Kinugawa S & Tsutsui H (2015). AST-120 ameliorates lowered exercise capacity and mitochondrial biogenesis in the skeletal muscle from mice with chronic kidney disease via reducing oxidative stress. *Nephrol Dial Transplant* in press.

Pal R, Palmieri M, Loehr JA, Li S, Abo-Zahrah R, Monroe TO, Thakur PB, Sardiello M & Rodney GG (2014). Src-dependent impairment of autophagy by oxidative stress in a mouse model of Duchenne muscular dystrophy. *Nat Commun* 5, 4425.

Paul PK, Bhatnagar S, Mishra V, Srivastava S, Darnay BG, Choi Y & Kumar A (2012). The E3 ubiquitin ligase TRAF6 intercedes in starvation-induced skeletal muscle atrophy through multiple mechanisms. *Mol Cell Biol* 32, 1248-1259.

Plomgaard P, Penkowa M & Pedersen BK (2005). Fiber type specific expression of TNF-alpha, IL-6 and IL-18 in human skeletal muscles. *Exerc Immunol Rev* 11, 53-63.

Poylin V, Fareed MU, O'Neal P, Alamdari N, Reilly N, Menconi M & Hasselgren PO (2008). The NF-kappaB inhibitor curcumin blocks sepsis-induced muscle proteolysis. *Mediators Inflamm* 2008, 317851.

Rommel C, Bodine SC, Clarke BA, Rossman R, Nunez L, Stitt TN, Yancopoulos GD & Glass DJ (2001). Mediation of IGF-1-induced skeletal myotube hypertrophy by PI(3)K/Akt/mTOR and PI(3)K/Akt/GSK3 pathways. *Nat Cell Biol* 3, 1009-1013.

Sharma S, Chopra K & Kulkarni SK (2007). Effect of insulin and its combination with resveratrol or curcumin in attenuation of diabetic neuropathic pain: participation of nitric oxide and TNF-alpha. *Phytother Res* 21, 278-283.

Suga T, Kinugawa S, Takada S, Kadoguchi T, Fukushima A, Homma T, Masaki Y, Furihata T, Takahashi M, Sobirin MA, Ono T, Hirabayashi K, Yokota T, Tanaka S, Okita K & Tsutsui H (2014). Combination of exercise training and diet restriction normalizes limited exercise capacity and impaired skeletal muscle function in diet-induced diabetic mice. *Endocrinology* 155, 68-80.

Takada S, Hirabayashi K, Kinugawa S, Yokota T, Matsushima S, Suga T, Kadoguchi T, Fukushima A, Homma T, Mizushima W, Masaki Y, Furihata T, Katsuyama R, Okita K & Tsutsui H (2014). Pioglitazone ameliorates the lowered exercise capacity and impaired mitochondrial function of the skeletal muscle in type 2 diabetic mice. *Eur J Pharmacol* 740, 690-696.

Takada S, Kinugawa S, Hirabayashi K, Suga T, Yokota T, Takahashi M, Fukushima A, Homma T, Ono T, Sobirin MA, Masaki Y, Mizushima W, Kadoguchi T, Okita K & Tsutsui H (2013). Angiotensin II receptor blocker improves the lowered exercise capacity and impaired mitochondrial function of the skeletal muscle in type 2 diabetic mice. *J Appl Physiol (1985)* 114, 844-857.

Tikoo K, Meena RL, Kabra DG & Gaikwad AB (2008). Change in post-translational modifications of histone H3, heat-shock protein-27 and MAP kinase p38 expression by curcumin in streptozotocin-induced type I diabetic nephropathy. *Br J Pharmacol* 153, 1225-1231.

von Haehling S, Genth-Zotz S, Anker SD & Volk HD (2002). Cachexia: a therapeutic approach beyond cytokine antagonism. *Int J Cardiol* 85, 173-183.

543 Wang Q, Guo T, Portas J & McPherron AC (2015). A soluble activin receptor type IIB does not
544 improve blood glucose in streptozotocin-treated mice. *Int J Biol Sci* 11, 199-208.
545
546 Wang X, Hu Z, Hu J, Du J & Mitch WE (2006). Insulin resistance accelerates muscle protein
547 degradation: Activation of the ubiquitin-proteasome pathway by defects in muscle cell
548 signaling. *Endocrinology* 147, 4160-4168.
549
550 Wang XH, Hu J, Du J & Klein JD (2007). X-chromosome linked inhibitor of apoptosis protein inhibits
551 muscle proteolysis in insulin-deficient mice. *Gene Ther* 14, 711-720.
552
553 Whitman SA, Long M, Wondrak GT, Zheng H & Zhang DD (2013). Nrf2 modulates contractile and
554 metabolic properties of skeletal muscle in streptozotocin-induced diabetic atrophy. *Exp Cell*
555 *Res* 319, 2673-2683.
556
557 Wray CJ, Mammen JM, Hershko DD & Hasselgren PO (2003). Sepsis upregulates the gene expression
558 of multiple ubiquitin ligases in skeletal muscle. *Int J Biochem Cell Biol* 35, 698-705.
559
560 Zuo L, Hallman AH, Roberts WJ, Wagner PD & Hogan MC (2014). Superoxide release from
561 contracting skeletal muscle in pulmonary TNF-alpha overexpression mice. *Am J Physiol*
562 *Regul Integr Comp Physiol* 306, R75-81.
563
564
565

Figure Legends

Figure 1 **Skeletal Muscle Atrophy in DM mice.** (**A**) Blood glucose level, (**B**) insulin level, (**C**) change in body weight, (**D**) rectus femoris weight, (**E**) gastrocnemius weight, (**F**) soleus muscle weight, (**G**) representative myocyte cross section of skeletal muscle stained with hematoxylin and eosin, (**H**) the summary data of myocyte cross-sectional area from Control, Control+Curcumin, Diabetes mellitus (DM), and DM+Curcumin mice (n=10 each). Scale bar: 50 μm. Data are means ± SEM. **P*<0.05 vs. Control, †*P*<0.05 vs. DM.

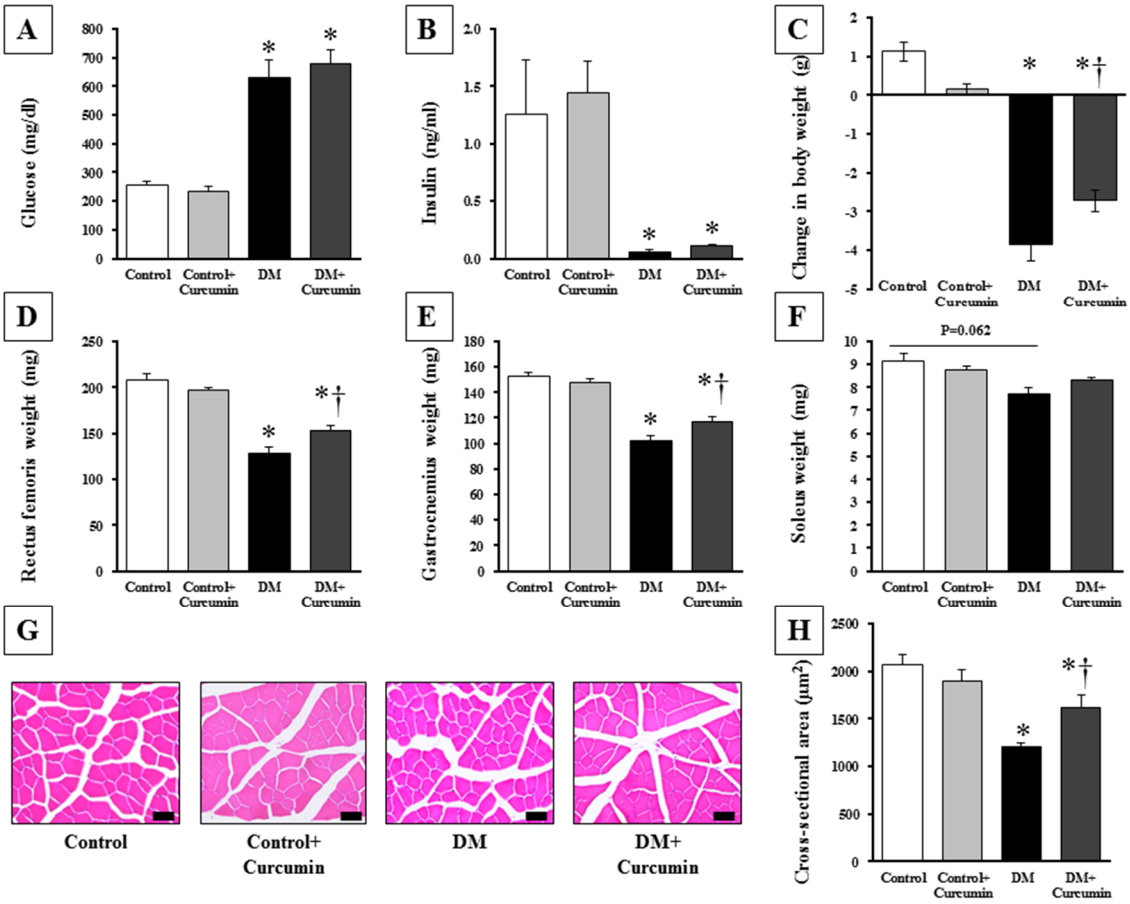

Figure 2 Curcumin Ameliorates Ubiquitination of Skeletal Muscle in DM mice. (**A**) Representative western blot analysis and (**B**) the summary data of ubiquitin-conjugated protein, and gene expression of muscle-specific E3 ubiquitin ligase, (**C**) Atrogin-1/MAFbx and (**D**) MuRF1 in skeletal muscle from Control, Control+Curcumin, DM and DM+Curcumin mice (n=6 each). Data are means ± SEM. **P*<0.05 vs. Control, †*P*<0.05 vs. DM. MAFbx, Muscle Atrophy F-box; MuRF1, muscle ring finger 1.

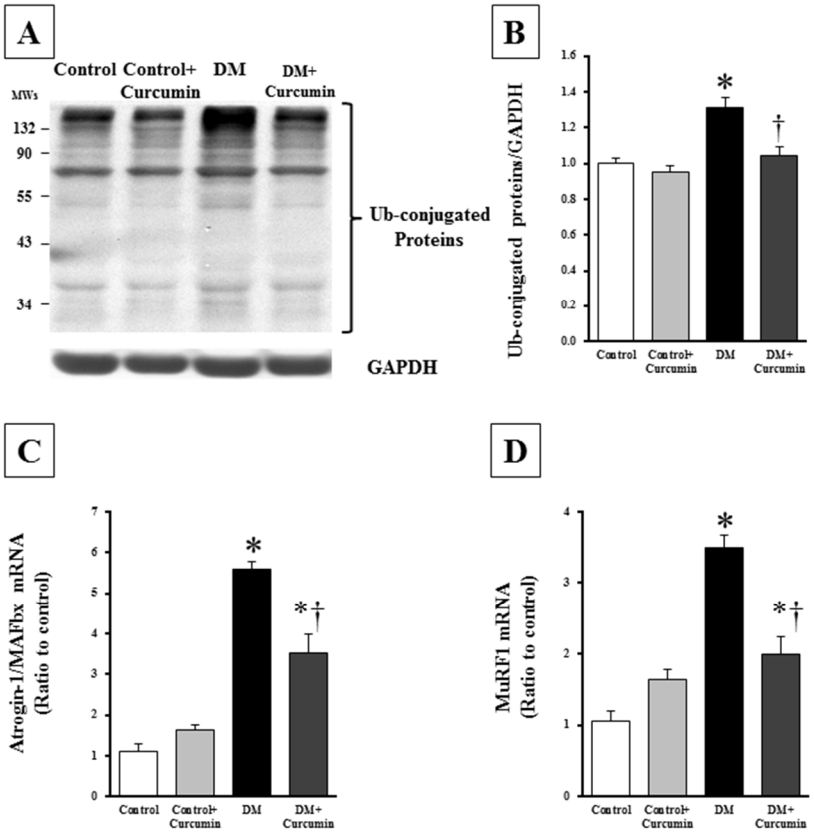

Figure 2

Figure 3 Curcumin Suppresses Inflammatory Cytokines and Oxidative Stress in the Skeletal Muscle in DM mice. Gene expression of inflammatory cytokines, (**A**) TNF-α, and (**B**) IL-1β in skeletal muscle and (**C**) TNF-α and (**D**) IL-1β in serum and (**E**) O_2^- production and (**F**) TBARS in skeletal muscle from Control, Control+Curcumin, DM, and DM+Curcumin (n=5-6 each). Data are means ± SEM. *P<0.05 vs. Control, †P<0.05 vs. DM. O2-, superoxide anion; TBARS, thiobarbituric acid reactive substances; TNF-α, tumor necrosis factor-alpha, IL-1β, interleukin-1 beta.

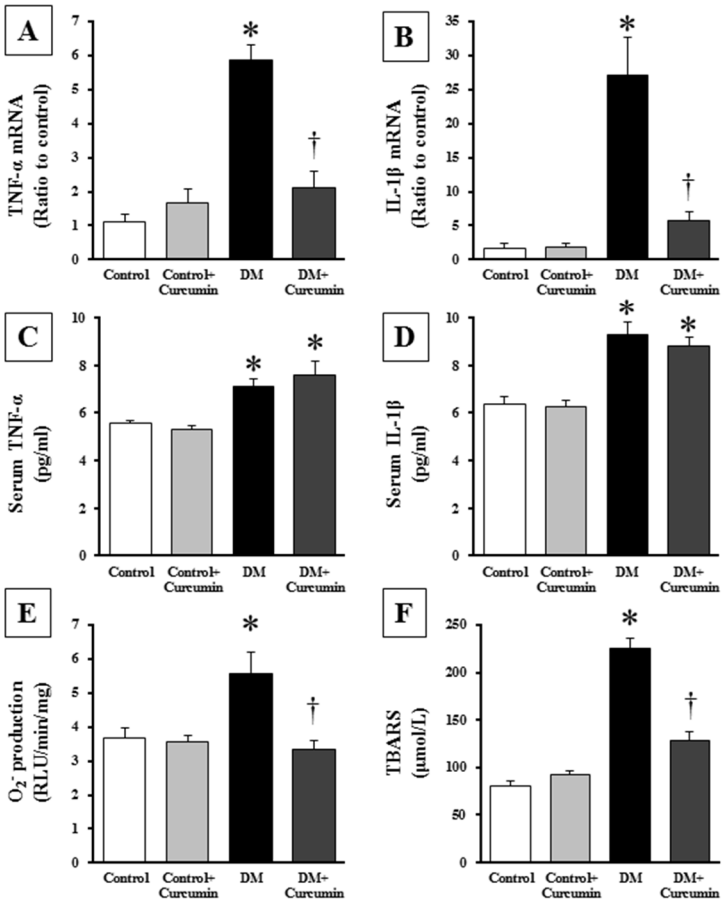

Figure 3

608 **Figure 4 Curcumin Inhibits NFκB activation but not Apoptosis and Autophagy in Skeletal**
609 **Muscle of DM mice.** (**A**) The summary data of NFκB p65 activation, (**B**), Ser253 p-FoxO3a, (**C**)
610 Thr32 p-FoxO3a, (**D**) cleaved caspase-3, (**E**) Atg12-Atg5, (**F**) LC3II in skeletal muscle from Control,
611 Control+Curcumin, DM, and DM+Curcumin mice (n=6-10 each). Data are means ± SEM. **P*<0.05 vs.
612 Control, †*P*<0.05 vs. DM. NFκB, nuclear factor-kappa B; FoxO, forkhead box O; Atg, autophagy-
613 related gene.

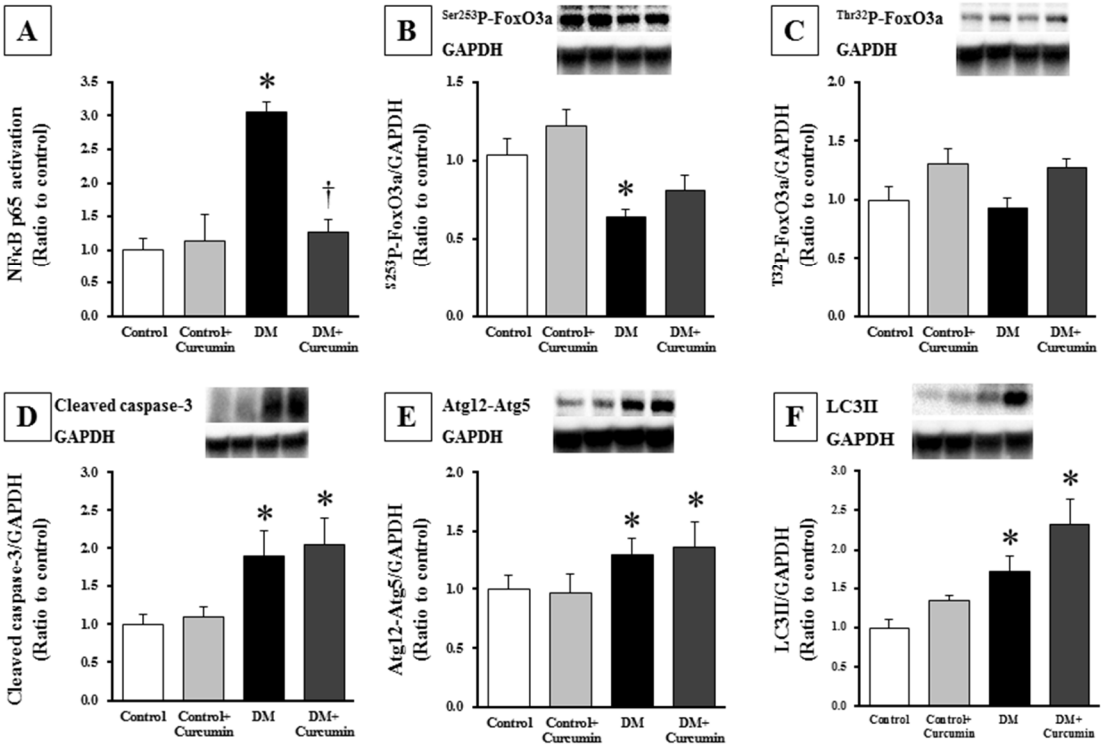

614 **Figure 4**

615

616

617

618

619

620

621

622 **Figure 5 Curcumin does not Affect Protein Synthesis in Skeletal Muscle in DM mice.** (**A**)
623 Circulating and (**B**) muscle IGF-1, (**C**) representative bands of western blot and (**C**) the summary data
624 of (**D**), Ser473 p-Akt, (**E**), Thr308 p-Akt, (**F**), Ser2448 p-mTOR, (**G**) Thr389 p-p70S6K, (**H**) p70S6K,
625 and (**I**) myostatin in skeletal muscle from Control, Control+Curcumin, DM and DM+Curcumin mice
626 (n=8-10 each). Data are means ± SEM. **P*<0.05 vs. Control. IGF, insulin-like growth factor; mTOR,
627 mammalian target of rapamycin.

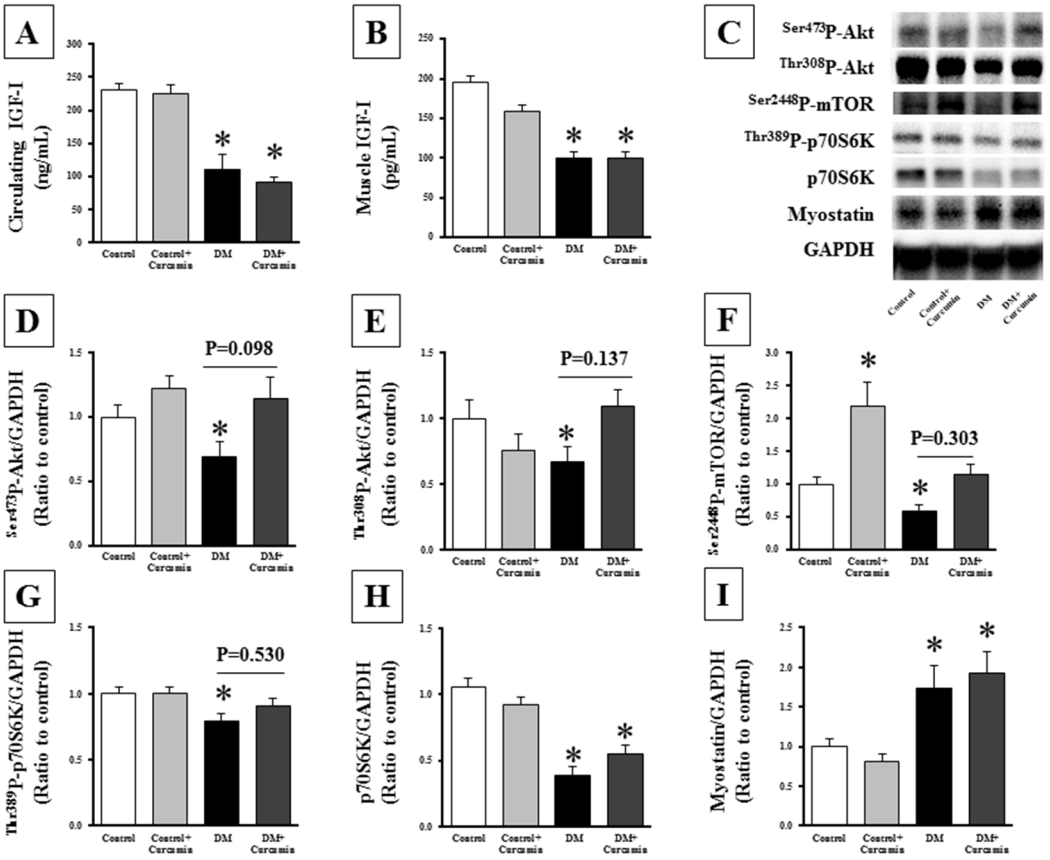

Figure 5

628